




## Evaluating the Effect of Thermal Shock on the Development of Micro-cracks in Granitoids Using Capillary Water Absorption Test and P-wave velocity Test

Leila Ahmadi <sup>1</sup>, Mohhamad Hosein Ghobadi <sup>1</sup>, \*, Ali Asghar Sepahi Garoo <sup>1</sup> , Leili Izadi Kian <sup>1</sup>, Seiede Razie Jafari <sup>2</sup>

<sup>1</sup> Department of Geology, Faculty of Science, Bu -Ali Sina University, Hamedan, Iran

<sup>2</sup> Department of geology, Payame Noor University, PO BOX 19359-3697, Tehran, Iran

Received: 29 August 2022, Revised: 14 December 2022, Accepted: 06 January 2023

© University of Tehran

### Abstract

Microcracks play an essential role in controlling rocks' physical and mechanical properties and thus are a vast research subject in engineering geology. The present study aimed to investigate microcracks developed in granitoids. Thermal shock at four temperatures of 250, 450, 650, and 850°C was applied to induce microcrack in granitoids. The rate of microcracks development and their effect on the physical properties of the rocks were assessed using the measurement of the P-waves velocity and capillary water absorption test. Both tests showed that the thermal shock, even in one cycle, has developed micro cracks. Moreover, the increased rate in effective porosity and total porosity of granitoids due to the growth of microcracks would estimate by the capillary water absorption test. This study showed that microcracks development directly relates to the increase in temperature at the thermal shock. The capillary water absorption test could measure the granitoids porosity as well as the water absorption and retention in the induced microcracks. These two tests could investigate microcracks development from two different points of view. The p-wave velocity estimates the propagation of different types of microcracks, while the capillary absorption test evaluates the connected microcracks. The effective porosity differently affects the rock mass efficiency in varied projects. Finally, total porosity and effective porosity are developed independently of each other through thermal-induced micro-cracks.

**Keywords:** Micro-Crack; Thermal Shock; Capillary Water Absorption; Speed Of Sound; Granitoid.

### Introduction

Microcracks in the rock are generated due to many natural and unnatural factors. Such factors accelerate chemical or physical weathering and microcracks development, so destroying the primary structures of the rock (Zhang et al., 2016). Investigating microcracks in rocks and their impact on physical, mechanical, and engineering geological features had been the focus of many researchers in the last few decades (Gomah et al., 2021). The formation of microcracks, also the factors expanding them, affect the physical properties and mechanical behavior of rocks. These factors include alternate cycles of heating and cooling, microwaves, alternate cycles of freezing and thawing, and crystallization of water or salts in the pores of the rock (Xu et al., 2019; Zhao et al., 2020). In geothermal systems, landfills of toxic and radioactive wastes or shale gas extraction, these factors are artificially created and cause microcracks (Darot et al., 1992; Sousa et al., 2005; Freire et al., 2016; Wang et al., 2016; Yin et al., 2019; Gue et al.,

\* Corresponding author e-mail: m.ghobadi@basu.ac.ir

2021; Zhang et al., 2021).

In some cases, microcracks are investigated and created to facilitate engineering drilling (Rossi et al., 2018) and mining projects targeted grinding of mineral ores (Niko et al., 2020), or storage and accumulation of carbon dioxide in geological formations (Aman et al., 2018). In the geothermal system, the cold water injection cycle, the heat exchange between the rock mass and the water, and the hot water extraction occur alternately in the rocks. In this system, the rate of creation and also characteristics of microcracks, strongly affect the continuity of the geothermal system. On the other hand, there are many natural microcracks in the rock, and factors such as heat cause their development and the formation of new microcracks (Chacki et al., 2008; Chanrasekharam et al., 2018). Granitoids are amongst the most abundant rocks in the crust and the most suitable rocks for generating geothermal energy and nuclear landfills (Olasolo et al., 2016; Yin et al., 2019). For these reasons, the study of granitoids and the type and extent of their behavior changes in response to thermal shock has been the subject of many recent studies in the field of granitoid (Kumari et al., 2019; Gomah et al., 2022; Costa et al., 2021; Khan & Sajid, 2023).

Although granitoids are usually considered homogeneous and isotropic rocks, fresh rocks always have some microcracks. In this respect, the formation of new micro cracks due to external factors is partially affected by previous microcracks (Sano & Kudo, 1992; Takemura et al., 2003; Nara et al., 2011). The presence of primary and induced cracks in the rock could be estimated using various methods. In geological studies, the P-wave velocity measurement method for estimating microcracks is one of the efficient, appropriate, low-cost, fast, and non-destructive methods (Nicco et al., 2018; Swanson et al., 2020; Gao et al., 2022). Measuring the P-wave velocity before and after thermal shock and comparing the results provide realistic estimates (Darot et al., 1992; Nasserri et al., 2007; Blake & Faulkner, 2016; Zhu et al., 2017; Ge et al., 2022).

Thermal shock increases the porosity (Alm et al., 1985; Humand- Etienne & Houpert, 1989; meng et al., 2020; Wong et al., 2020) and consequently increases water absorption (Yu et al., 2021). The shape, type, size, and homogeneity connection mode of cavities and pores in rock greatly influence water absorption and other fluids (Darot et al., 1992; Ortega & Marrett, 2000). Rock durability is extremely affected by the speed and quantity of capillary water absorption and its retention in rock pores (Tomasic et al., 2011), therefore it is a good indicator for estimating the cracks or microcracks development in granitoids (Vazquez et al., 2010). In granitoids, porosity development is mainly in the cracks or micro-cracks form, so water absorption in this type of porosity is due to capillary water absorption. Other petrographic factors such as the type, size, distribution, position of the minerals, and the homogeneity of the rock are also effective in water absorption.

Porosity, cavities, and microcracks with a cross-section of 6 to 20  $\mu\text{m}$  can allow capillary water to rise by 3 to 10 m while those with a cross-section of 2 to 6  $\mu\text{m}$  may result in capillary water absorption to a height of 10 to 30 m. During the same period, the horizontal water movement is twice faster as the vertical water movement (Tomasic et al., 2011). Therefore, the capillary water absorption test could be used as an indicator of the presence of microcracks and the rate of their development in the rock.

The present study estimated induced thermal cracks and microcracks in three samples of coarse-grained granitoids from Iranian granitoids using p-wave velocity and capillary water absorption tests. In this research, microcrack induction was performed by heating rock and then shock by cold water. Finally, the obtained data were used as damage threshold and threshold for cracking and micro-cracking at induced temperatures.

### **Geological and lithological characteristics**

The rock samples were taken from the granitoids of three regions of Alvand, Hassan Rebat, and

Marivan, all located in the Sanandaj-Sirjan structural zone in western Iran (Fig. 1).

The samples were taken from coarse-grained and completely fresh rocks. Mineralogical studies using thin microscopic sections also showed that the rocks are fresh and non-weathered, according to their mineralogical properties. The mineralogical properties of the samples are summarized in Table 1. The mean size of constituent particles of rock was also estimated using the macroscopic specimens. The mean particle size of Alvand, Hassan Rebat, and Marivan samples was about 7 to 10 mm, 3 to 7 mm, and 1 to 3 mm, respectively. In terms of uniformity in macroscopic sample, the granite particle size of Hassan Rebat was more uniform than the others.

The presence of very large particles in Alvand granite caused a range of fine to coarse particles. Since the grains in the Marivan sample were generally finer, the particle size range was not wide. Fig. 2 shows samples of granites.

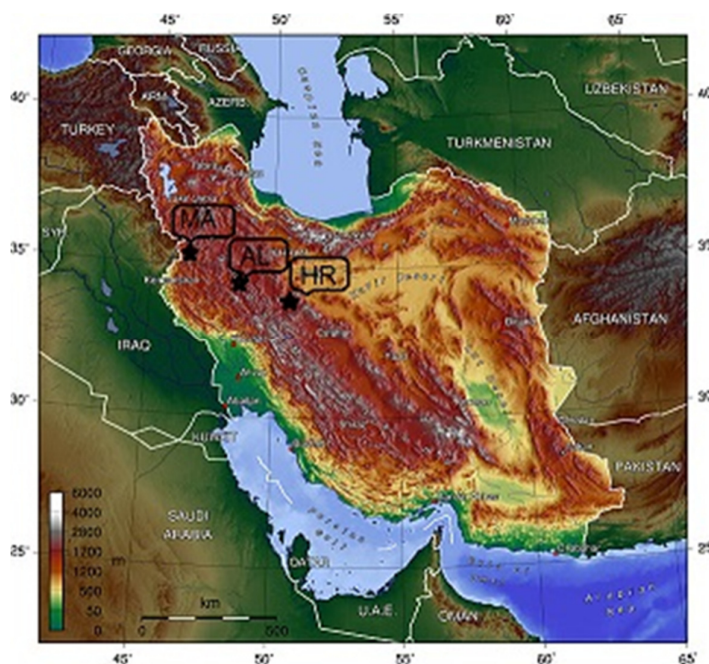
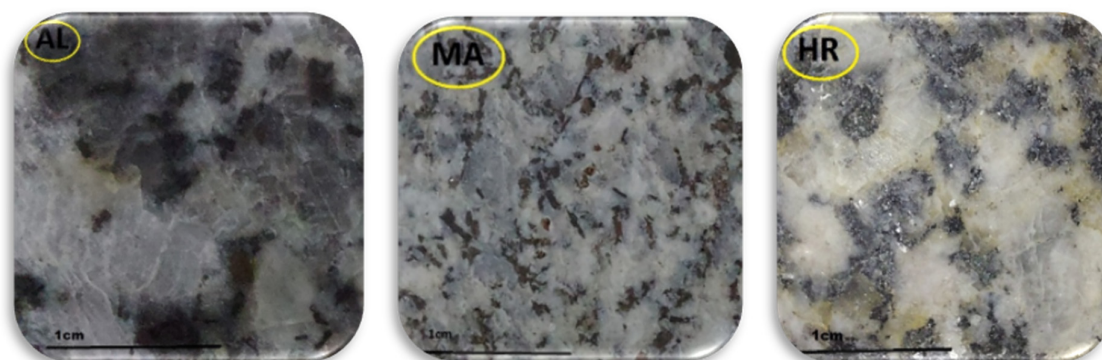


**Figure 1.** Map of Iran and location of sampling Marivan (MA), Alvand (AL), Hasan Rebat (HR)



Orthoclase: 5-12 mm  
Plagioclase: 2-7 mm  
Quartz: 4-7 mm  
Biotite: 1-3 mm

Orthoclase: 2-5 mm  
Plagioclase: 3-8 mm  
Quartz: 1-3 mm  
Biotite: 2-4 mm

Orthoclase: 4-10 mm  
Plagioclase: 2-6 mm  
Quartz: 4-7 mm  
Biotite: 1-3 mm

**Figure 2.** Hand samples of granites. Alvand (AL). Marivan (MA). Hasan Rebat (HR)

**Table 1.** Mineral's modal percent of granitoid samples

Minerals (modal percent) & sample name	Quartz	Plagioclase	Orthoclase	Biotite	Sphene	Sericite	Muscovite	Garnet	Chlorite	Hornblende
Alvand	23	17	37	13		4	5	1		
Marivan	37	28	21	11			1		2	
Hasan Rebat	38	18	26	10	1	2				5

## Method

The micro-crack induction method as follows: rock blocks were taken from three different areas, cores with 54 mm diameter were prepared using a coring- machine, then 5 individual group was selected from each granite samples. Granite samples with circular cross-sections were tested according to HRN EN test standard 1925; 1999 (natural rock test methods – determination of capillary water absorption coefficient) (Tomasic et al., 2011). The capillary water absorption was tested on one group of every fresh rock sample and the other four groups of samples were heated in laboratory furnace. The samples in the furnace were subjected to the desired heat for 2 h. After leaving the furnace, they were transferred to the cold water tank immediately. The municipal water was streaming to the tank until the sample temperature reached the temperature of tap water. After exiting the samples from the water tank, they were kept in the hothouse for 48 h at 50-60°C to dry. Afterward, they were kept at room temperature to perform the capillary test. The applied temperatures were 250, 450, 650, and 850°C. Fresh samples were exposed to maximum temperature of 60°C for drying. P-wave velocity test was performed before and after thermal shock, also before and after capillary water absorption test on every samples. Moreover, physical properties of the samples were determined before and after thermal shock.

## Tests and results

### *Determination of physical properties*

Physical characteristics of fresh and thermal-shocked samples were determined according to ISRM standard (Fahimifar & Soroush, 2001). The results of this test are presented in Table 2. Results showed the samples do not have a significant difference in volumetric mass values. Although the porosity in the Marivan sample significantly differed from the Alvand and Hassan Rebat samples, the density of rock grains(Gs) in Hassan Rebat differed a little from the others.

### *Determination of P- wave velocity (Vp)*

The p-wave velocity test using the PUNDIT6 machine was performed on granites in three perpendicular directions before and after thermal shock according to ISRM standards (Fahimifar & Soroush, 2001). Average of three direction Vp were calculated and Table 3 shows results of the p-wave velocity test of dry samples. Vp declined in the studied samples due to thermal shock, suggesting cracks and micro-cracks development in the samples. The rate of p-wave velocity drop in the samples was directly related to the increase in applied temperature. With increasing the applied heat, the speed drop percentage also increased. All samples showed a 90% drop in Vp after 850°C heat shock compared to the fresh state. In addition, the Vp drop rate corresponding to the 650°C thermal shock was close to the above value. However, in the

thermal shock of 450 and 250°C, the Vp drop was significantly less than 90%. Comparing the drop in speed due to the 250°C and 450°C thermal shock also shows a clear difference in Vp drop. The results are summarized in Table 3. The Marivan and Alvand samples had the lowest and highest Vp among fresh samples, respectively. Besides, Marivan has the most percentage of Vp drop after heat 850°C shock and Alvand has the least percentage of Vp drop after 250°C heat shock.

### Determination of capillary water absorption

Capillary water absorption tests were carried out on samples according to HRN EN 1925; 1999 standard (Tomasik et al., 2011). The results of these tests on fresh and thermal-shocked samples are shown in Figs. 4,5,6. These results were examined in three ways.

**Table 2.** Physical properties of granitoid samples

Name	Number of data =29	Dry density (gr/cm <sup>2</sup> )	Saturated density (gr/cm <sup>2</sup> )	Effective Porosity (%)	Void Index <sup>1</sup> (%)	Grain Density
<b>Alvand</b>	Mean	2.663	2.670	0.73	0.24	2.762
	STDV	0.011	0.011	0.08	0.02	0.033
<b>Hasan Rebat</b>	Mean	2.644	2.653	0.88	0.29	2.674
	STDV	0.011	0.009	0.27	0.15	0.024
<b>Marivan</b>	Mean	2.652	2.663	1.12	0.36	2.755
	STDV	0.006	0.005	0.13	0.01	0.03

<sup>1</sup>The void index is determined by quick water absorption method.

**Table 3.** Sound velocity in granitoids before and after thermal shock

Name	Number of data = 20	Sound velocity in fresh sample before shock (m/s)	Sound velocity in sample after shock (m/s)	Sound speed drop percentage (%)	Speed ratio (before to after thermal shock)
<b>Marivan 250</b>	Mean	6215	4854	22	1.3
	STDV	618	337	4	0.1
<b>Hasan Rebat 250</b>	Mean	6376	4724	25	1.3
	STDV	1049	518	8	0.1
<b>Alvand 250</b>	Mean	7647	6092	20	1.3
	STDV	631	918	9	0.1
<b>Marivan 450</b>	Mean	6210	3298	47	1.9
	STDV	656	269	5	0.2
<b>Hasan Rebat 450</b>	Mean	6925	2798	59	2.5
	STDV	621	235	4	0.2
<b>Alvand 450</b>	Mean	7642	3939	49	2.0
	STDV	805	1050	12	0.4
<b>Marivan 650</b>	Mean	5859	867	85	7.1
	STDV	701	181	4	1.8
<b>Hasan Rebat 650</b>	Mean	7558	1135	85	6.7
	STDV	991	102	2	0.8
<b>Alvand 650</b>	Mean	8028	1147	86	8.2
	STDV	914	554	6	2.8
<b>Marivan 850</b>	Mean	6005	449	92	13.6
	STDV	571	62	1	2.2
<b>Hasan Rebat 850</b>	Mean	7476	927	87	8.1
	STDV	1332	132	2	1.3
<b>Alvand 850</b>	Mean	7453	764	90	12.3
	STDV	630	396	5	5.5

- 1-Change in capillary water absorption in 72 h due to thermal shock in granites
- 2-Change in the velocity of capillary water absorption due to thermal shock in granites
- 3-Change in the retention time of capillary water due to thermal shock in granites

*Change in capillary water absorption in 72 h due to thermal shock in granites*

The quantity of capillary water absorption in 72 h in all three samples is directly related to the amount of thermal shock applied. Samples subjected to higher thermal shock show higher capillary water absorption, while the lowest is observed in fresh specimens. This value varies from approximately 170 g/m<sup>2</sup> in the fresh sample to 3000 g/m<sup>2</sup> in the shocked specimen during 72 h. The results show a clear difference between the 72-h capillary water absorption at thermal shock above and below 500°C. All three samples showed much higher capillary absorption after the thermal shock of more than 500°C, suggesting micro-crack development was accelerated by more than 500°C thermal shock.

Comparing the capillary water absorption of three samples in different heat shocks revealed that since the Marivan sample has higher porosity (effective) in the fresh state (without thermal shock), it has more capillary water absorption than the other two samples. However, after the thermal shock of 250°C, increasing the quantity of capillary water absorption in all three samples, the amount of absorption gets closer to each other. The porosity in the Marivan sample provided the conditions for the expansion of particles and minerals. The existing porosity partially controlled the development of micro-cracks; nevertheless, this procedure did not observe in the other two samples.

In 450°C samples of Hassan Rebat and Marivan, the water absorption was significantly increased compared to the Alvand sample. Also, in both specimens, the increase in absorption doubled compared to the 250°C thermal shock. Meanwhile, in the Alvand sample, the amount of capillary water absorption is not different from 250°C. This trend has shown in Fig. 3.

In three samples, the increase in capillary water absorption of 650°C is more than the 450°C temperature shock, but this increase has highly noticed in the 650°C Alvand sample. In this regard, this sample's increase in water absorption is eight times the 450°C temperature, while it is 3 to 4 times in the two specimens. It seems that cracks development in the Alvand sample is at the grain boundary up to 450°C, exceeding which it suddenly expands into the grains (Gomah et al., 2021). However, in the Hassan Rebat sample, crack development began and continued uniformly throughout the rock structure. The noteworthy point in this regard is the difference in the effect of temperature of 650°C compared to 450°C.

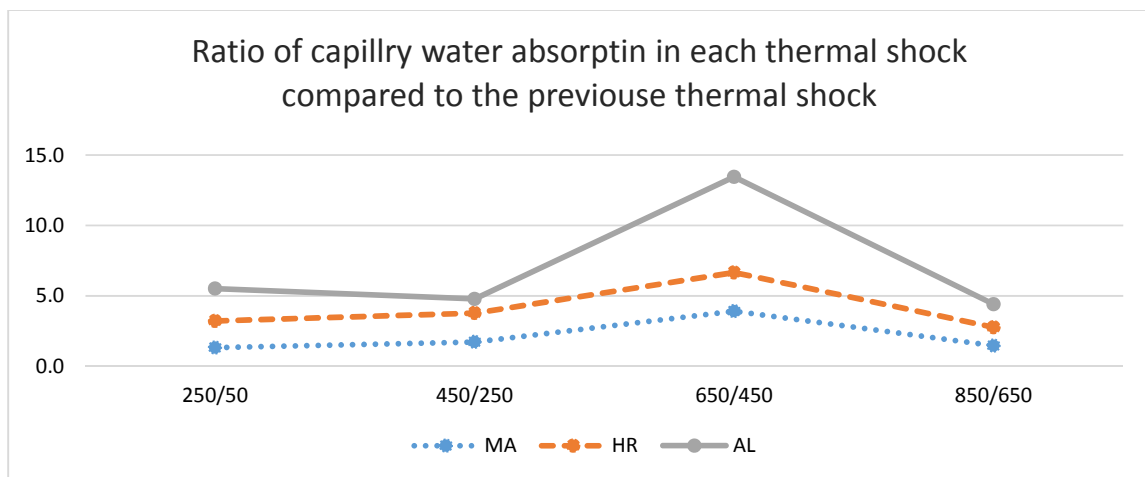


**Figure 3.** The ratio of capillary water absorption in each temperature shock compared to the previous temperature shock

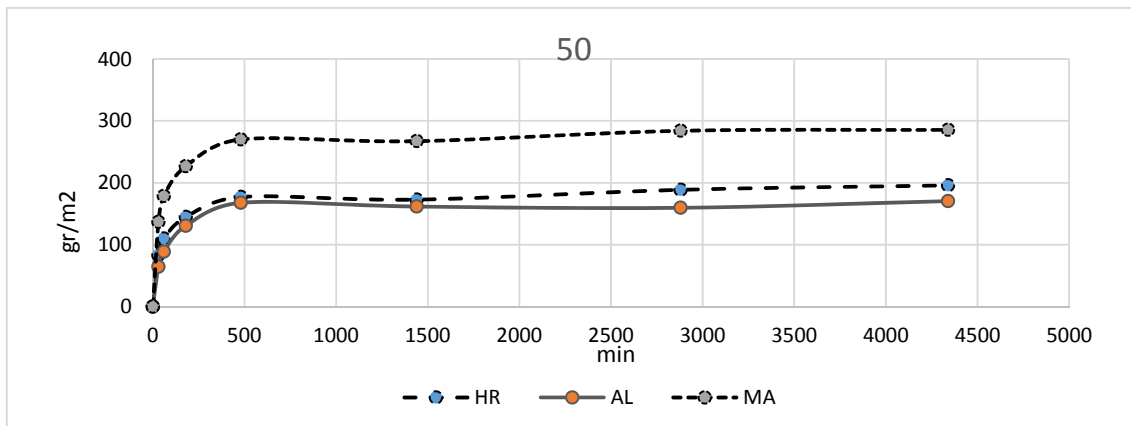


Figure 4. Capillary water absorption in fresh sample

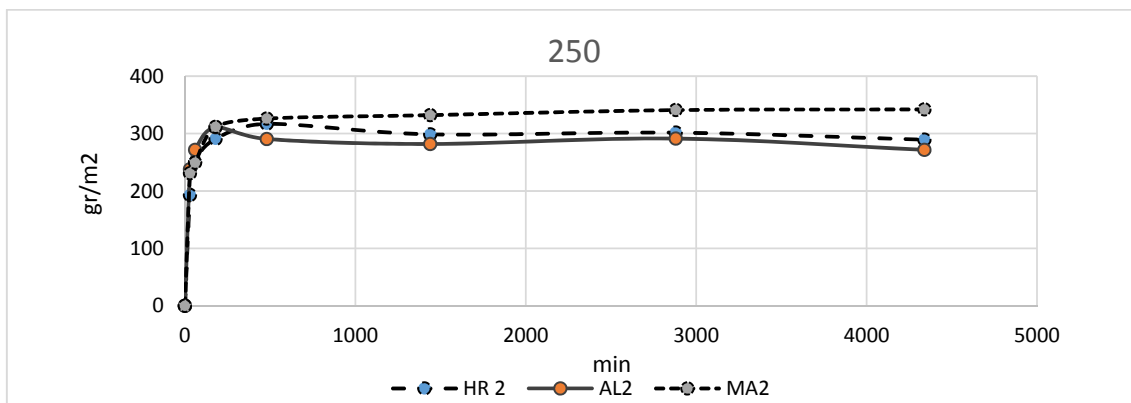


Figure 5. Capillary water absorption in granitoids sample after 250 C thermal shock

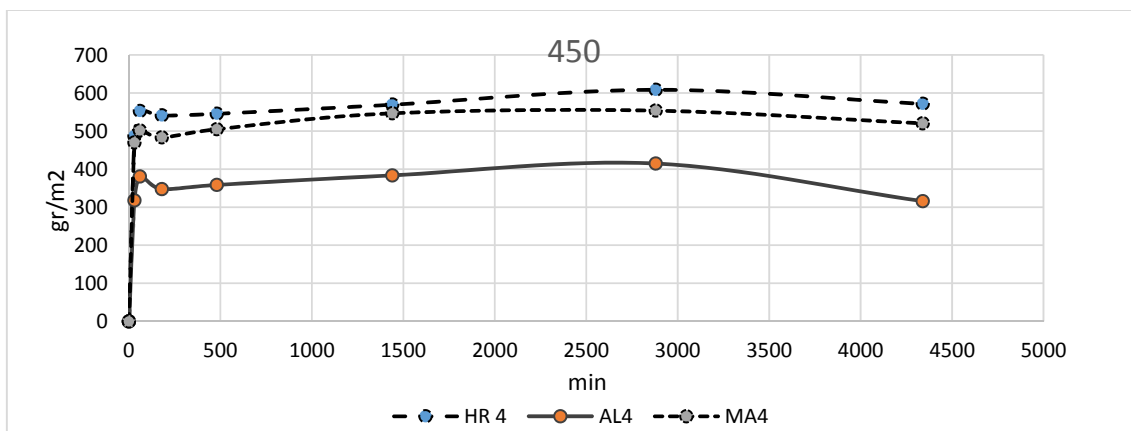


Figure 6. Capillary water absorption in granitoids sample after 450C thermal shock

Table 4 presents capillary water absorption due to thermal shock compared to fresh capillary absorption. In the granite samples after the highest thermal shock (850°C), capillary water absorption in the Alvand sample increased by 26 times, while in two other specimens, the increases were 13 and 14 times. Although all specimens are coarse-grained granites, the average particle size affects the rate of crack development. The smallest mean particle size and the most porosity have been observed in Marivan, and the Alvand sample had the coarsest grains and the most minor porosity.

After 850°C temperature shock, Alvand and Marivan samples have the same capillary



absorption. Meanwhile, in the fresh state, the lowest amount belonged to the Alvand, and the highest amount belonged to the Marivan sample. Comparing capillary water absorption in two states (after 650°C and 850°C thermal shock) revealed that all three samples have approximately 1.5 times increase in the capillary water absorption, suggesting that crack development has continued. However, the increase in capillary absorption at this stage compared to the previous thermal-shock stage indicates that the crack development, especially in the Alvand sample, is close to its final level, and capillary water absorption diagrams are very close to the horizontal.

*Change in the velocity of capillary water absorption due to thermal shock in granites*

Fig. 4,5,6,7,8 show the capillary water absorption trend in each sample separately sorted by shock temperature. In the capillary water absorption test, the amount of water absorption is calculated in gr/m<sup>2</sup> & s<sup>0.5</sup>. In these diagrams, water absorption is determined by the ascending state, water retention by the horizontal state, and release of absorbed water by the descending form of the graph. In inspect of the capillary water absorption process, three factors were considered: absorption velocity, absorption amount, and water retention time.

**Table 4.** The average capillary water absorption is 72 hours after each thermal shock compared to the fresh state

Temperature applied for thermal shock		50	250	450	650	850
Sample name	Marivan	1	1	2	9	13
	Hasan Rebat	1	2	4	11	14
	Alvand	1	2	2	16	26

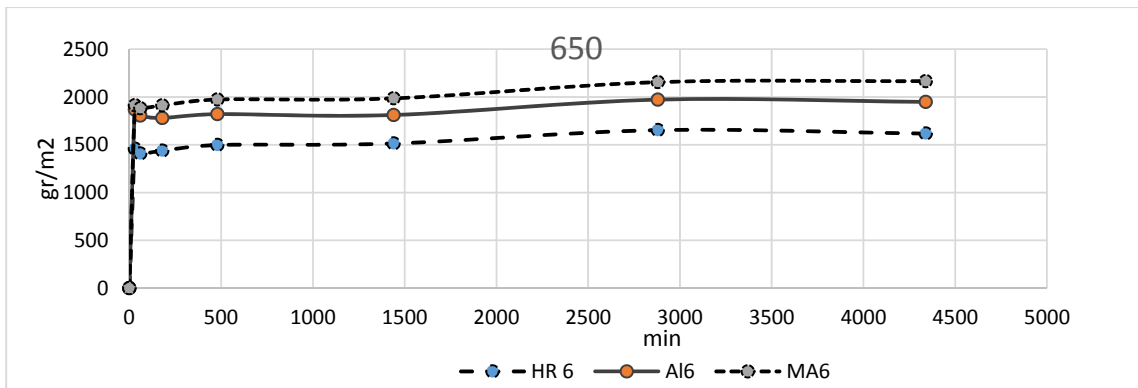


**Figure 7.** Capillary water absorption in granitoids sample after 650 C thermal shock

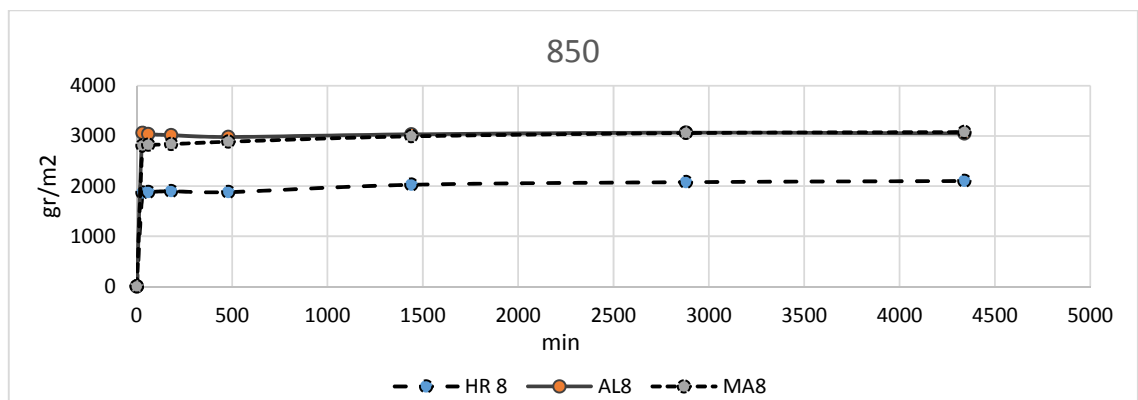


**Figure 8.** Capillary water absorption in granitoids sample after 850 C thermal shock



The capillary water absorption test results showed that the maximum absorption velocity was in the first 30 min. The absorption rate sharply decreased in the second 30 min, which continued in the following hours. Finally, the sample reached the release stage or the end of water retention. The decreasing trend in absorption velocity differed at different thermal shocks. Also, the absorption velocity is affected by the horizontal development of micro-cracks. Therefore, the examine the P-wave velocity in three directions in the samples and the capillary absorption speed provided a better view of the development of micro-cracks.

#### *Change in the retention time of capillary water due to thermal shock in granites*

Figs 9,10,11 show the capillary water absorption test results in three samples separately sorted by five temperature groups. In these diagrams, the process of absorption and retention, also the absorption velocity, could be identified. It must note that after the thermal shocks of more than 500°C, especially in the Alvand sample, some particles separated from the rock during the test, which can cause a slight error in estimating capillary absorption.

In fresh samples, all specimens retained water for up to 8 h, but they showed signs of water release after this period. According to the negative numbers that indicate the release of water in the relevant time, it is observed that granite samples show a shorter retention time as the thermal shock rises, which is not a regular but detectable process. This trend seems to be related to the average particle size of the samples, which could affect the cross-sectional expanse of the micro-cracks. The Marivan sample with the smallest average particle size showed a higher retention time in all thermal shocks, and the Alvand sample with the largest average particle size showed a shorter retention time. A shorter retention time means that the crack development has surpassed that of micro-cracks. As the cross-section of the micro-cracks gets closer to 2 to 6  $\mu\text{m}$ , the velocity of water absorption and movement increases in the vertical direction, and at the same time, the speed in the horizontal direction is twice. Cracks have less retention time than micro-cracks because the water in them can return due to the dominance of gravity over capillary suction. The greater the thermal shock, the more difference between the minimum and maximum temperatures, and more and wider cracks are formed in them (Siegsmund et al., 2018; Darot et al., 1992; Khan & Sajid, 2023).

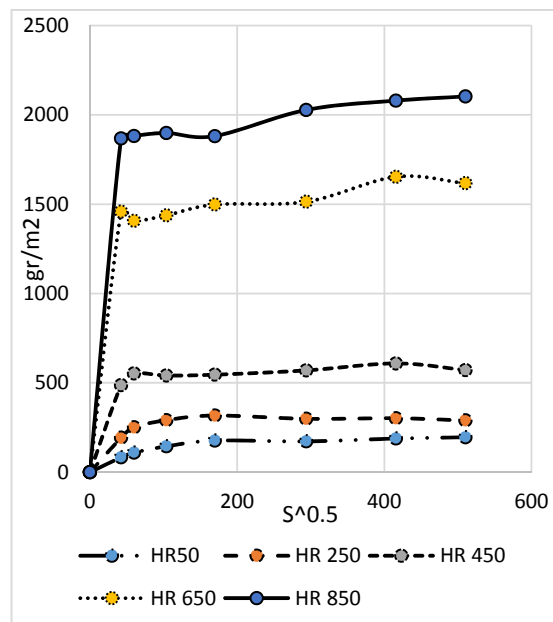


**Figure 9.** Capillary water absorption in Alvand granite after 5 different thermal shocks

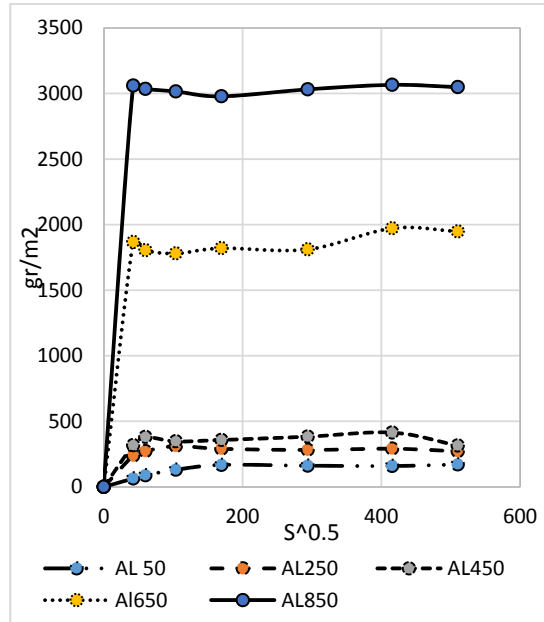


Figure 10. Capillary water absorption in Hasan Rebat granite after 5 different thermal shocks

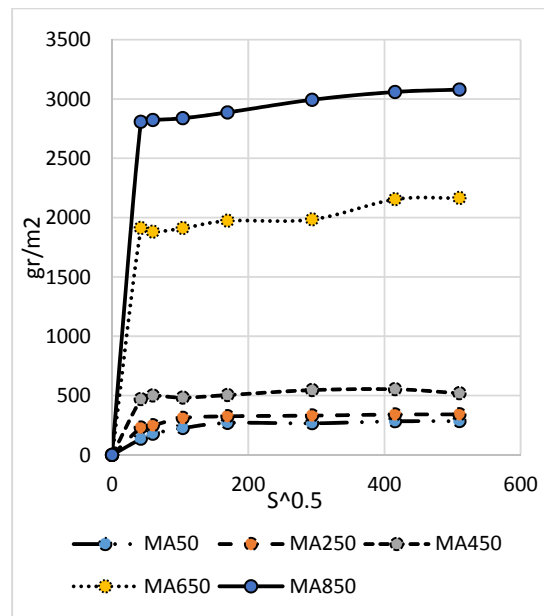


Figure 11. Capillary water absorption in Marivan granite after 5 different thermal shocks

An individual mineral has a specific heat capacity and homogeneous behavior against heat and shock. The Alvand sample contains coarse minerals that they have placed next to other finer minerals with varying heat capacities. The shock causes numerous long micro-cracks to form at the boundary of this coarse mineral with a set of finer minerals, and wider cracks initiate by joining them in the frontier of that mineral (Such cracks have been identified in microscopic thin sections). This type of crack formation has decreased as the size of the minerals becomes uniform, and as the size of minerals becomes similar, the forming of micro-cracks surpasses the cracks. This issue is reflected in water retention so that in the Marivan sample, fine and uniform particles form an identical network of micro-cracks, because of this water retention time increment. In the Hassan Rebat sample, where the minerals are finer than in the Alvand sample, the water retention time is longer than the Alvand sample and less than the Marivan

sample. In all three fresh granite samples, the retention time is 72 hours. The 72 h retention time after thermal shock is observed in the Alvand 850°C sample and all Marivan samples except the 450°C specimen, retention time in the others were fallen off to 48 hours.

## Discussion

The results showed that the capillary water absorption test would evaluate the micro-crack development rate due to thermal shock. Effective porosity affects the amount of water absorption in fresh samples. But, by inducing micro-cracks through the thermal shock in granites, that was seen that the process of capillary water absorption takes a different form. The development of microcracks was so that affects the total volume of the sample and the amount of capillary water absorption shows interesting results, taking into account the porosity caused by the development of microcracks (Costa et al., 2021). Tables 5,6 show the results of the physical properties test on the samples before and after the thermal shock. Figs 12 to 14 show a comparison between the parameters of the tables. Fig. 12 indicates that the dry and saturation density of fresh and thermal-shocked granite samples change. Since the grain density had been measured in the samples and was constant during thermal shock tests, therefore the rock density decrease is derived from the samples volume increment due to thermal shock. The micro-cracks and cracks had developed due to thermal shock, so the cracks in samples were visible by the naked eye (Zhang et al., 2021). These cracks and micro-cracks will increase the volume and consequently decrease the density (Costa et al., 2021). The important point in these granite samples is that in the Hassan Rebat sample, the grain density(Gs), or in other words, the solid part of the rock, is very close to the dry and saturation density of the fresh rock, which means that the fresh sample has very few cracks and micro-cracks. A more difference between the grain density and the dry and saturated density in the fresh rock could be observed in the other two samples. This point is also reflected in the study of the total and effective porosity of the fresh sample of Hassan Rebat. The total and effective porosity in this sample are very close to each other, so the specimen is very dense and has low porosity. In fresh granites of Alvand and Marivan, the difference between grain density and dry and saturated density is more. The total porosity in Alvand fresh sample is about five times and in the Marivan sample about three times the effective porosity of these samples, indicating the existence of empty and unrelated spaces in them.

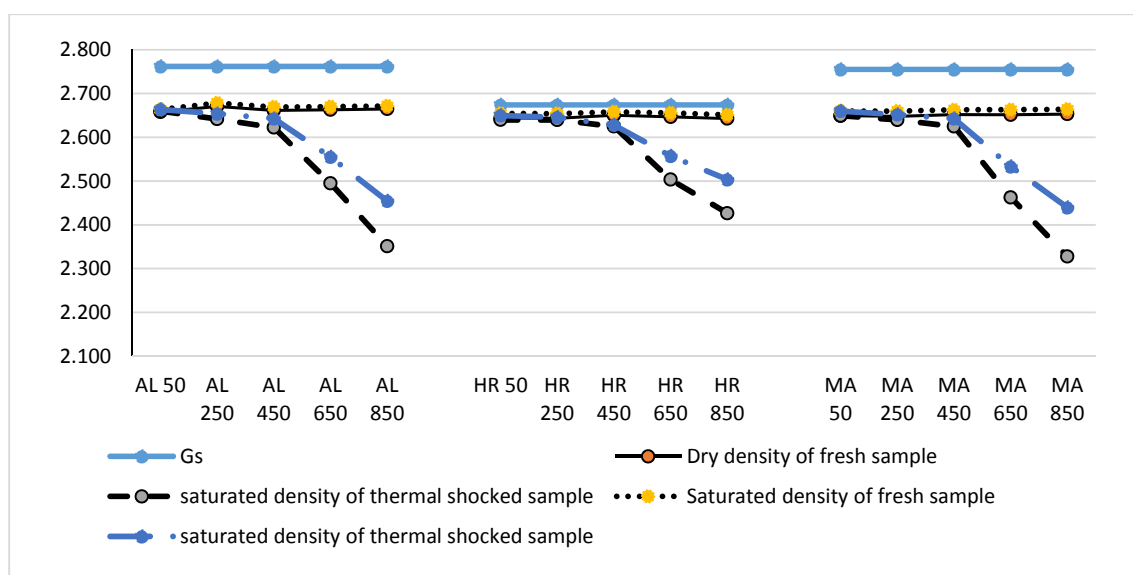


**Figure 12.** Density of sample before & after thermal shock. (Alvand granite AL – Hasan Rebat granite HR – Marivan granite MA)

**Table 5.** physical properties of granitoids before and after thermal shock (Alvand granite AL – Hasan Rebat granite HR – Marivan granite MA)

name	Gs	Dry density of fresh sample	Dry density of thermal shocked sample	Saturated density of fresh sample	saturated density of thermal shocked sample	Effective porosity of fresh sample	Effective porosity of thermal shocked sample	Porosity of fresh sample	Porosity of thermal shocked sample
AL50	2.762	2.658	2.660	2.664	2.664	0.75	0.75	3.77	3.77
AL250	2.762	2.671	2.642	2.678	2.654	0.78	1.19	3.31	4.31
AL450	2.762	2.661	2.622	2.669	2.643	0.80	2.01	3.65	4.98
AL650	2.762	2.663	2.495	2.670	2.555	0.72	5.77	3.58	9.42
AL850	2.762	2.665	2.351	2.672	2.455	0.69	10.34	3.52	14.92
HR50	2.674	2.644	2.640	2.655	2.650	0.75	0.75	3.77	3.77
HR250	2.674	2.644	2.640	2.654	2.646	0.78	1.19	3.31	4.31
HR450	2.674	2.650	2.625	2.658	2.628	0.80	2.01	3.65	4.98
HR650	2.674	2.647	2.504	2.656	2.557	0.72	5.77	3.58	9.42
HR850	2.674	2.643	2.427	2.651	2.504	0.69	10.34	3.52	14.92
MA50	2.755	2.649	2.649	2.660	2.660	1.15	1.15	3.83	3.83
MA250	2.755	2.648	2.640	2.660	2.652	1.18	1.24	3.89	4.13
MA450	2.755	2.652	2.625	2.663	2.643	1.11	1.78	3.75	4.75
MA650	2.755	2.651	2.463	2.663	2.533	1.19	7.04	3.76	10.60
MA850	2.755	2.653	2.328	2.664	2.440	1.10	11.27	3.70	15.60

**Table 6.** physical properties of granitoids before and after thermal shock. (Alvand granite AL – Hasan Rebat granite HR – Marivan granite MA)

name	Quick water absorption of fresh sample	Quick water absorption of thermal shocked sample	Saturated degree after CWA test	Water content after CWA test	Volume increase percentage	Ratio of porosity to effective porosity in fresh sample	Ratio of porosity to effective porosity in thermal shocked sample	Ratio of porosity in thermal shocked to fresh sample	Ratio of effective porosity in thermal shocked to fresh sample
AL50	0.039	0.039	18.4	0.26	0.00	5.1	5.0	1.0	1.0
AL250	0.034	0.045	20.3	0.33	1.02	4.3	3.6	1.3	1.5
AL450	0.038	0.052	27.3	0.51	1.30	4.5	2.5	1.4	2.5
AL650	0.037	0.104	67.6	2.52	5.82	5.0	1.6	2.6	8.0
AL850	0.036	0.175	64.4	4.00	10.41	5.1	1.4	4.2	15.1
HR50	0.011	0.011	58.4	0.24	0.00	1.3	1.3	1.0	1.0
HR250	0.012	0.014	59.1	0.31	0.23	1.1	1.4	1.2	1.0
HR450	0.009	0.024	72.6	0.65	1.45	1.1	1.2	2.7	2.4
HR650	0.010	0.068	72.0	1.83	5.49	1.1	1.2	6.2	6.0
HR850	0.012	0.100	64.0	2.35	8.41	1.4	1.2	7.8	9.0
MA50	0.040	0.040	24.1	0.35	0.00	3.3	3.3	1.0	1.0
MA250	0.040	0.043	28.7	0.45	0.23	3.3	3.3	1.1	1.0
MA450	0.039	0.050	34.5	0.62	0.96	3.4	2.7	1.3	1.6
MA650	0.039	0.119	60.6	2.54	7.21	3.2	1.5	2.8	5.9
MA850	0.038	0.185	57.4	3.84	13.51	3.4	1.4	4.2	10.2

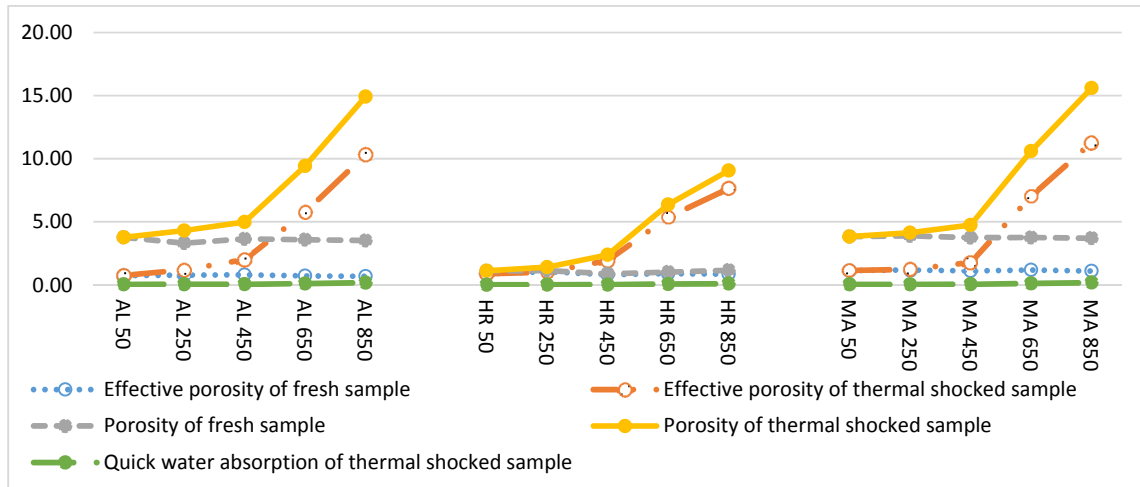


**Figure 13.** Porosity of sample before & after thermal shock. (Alvand granite AL – Hasan Rebat granite HR – Marivan granite MA)

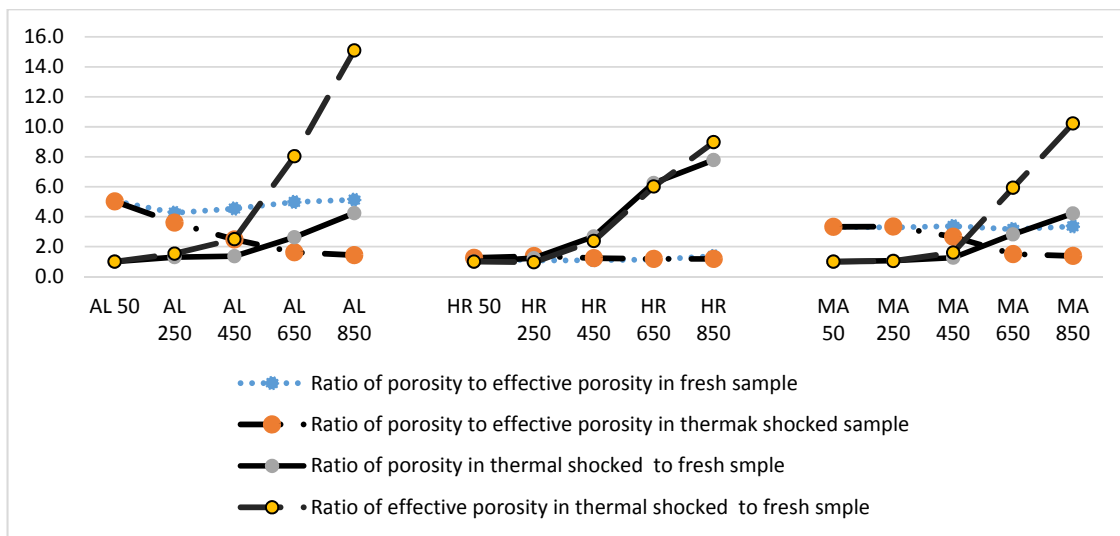


**Figure 14.** Ratio of porosities in samples before & after thermal shock. (Alvand granite AL – Hasan Rebat granite HR – Marivan granite MA)

The behavior of granite specimens after thermal shock can express in an overall look in this way: The effect of thermal shock on all samples is little up to 500°C, but with increasing temperature to more than 500°C, its effect on the physical properties of granites increases significantly (Costa et al., 2021; Gomah et al., 2021; Meng et al., 2020). Raising the temperature to more than 500°C causes a significant decrease in density (Gomah et al., 2022). The slightest reduction in density or increase in volume occurs in the Hassan Rebat sample, so the rate of cracks development and micro-cracks in this sample is less than in the others.

In the samples of Alvand and Marivan, where the initial total porosity was higher, the empty spaces, which are often linear in granites, formed weak surfaces against thermal shock. The minerals have expanded and retracted in these surfaces and developed more due to thermal shock.

Fig. 13 shows the increasing trend of total and effective porosity in fresh and thermal-shocked samples. Diagrams show that by increasing the thermal shock temperature, the effective and total porosity increase (Gao et al., 2022; Liu et al., 2022). When the temperature of thermal shock is below 500°C, this increase is significantly lesser than when its temperature

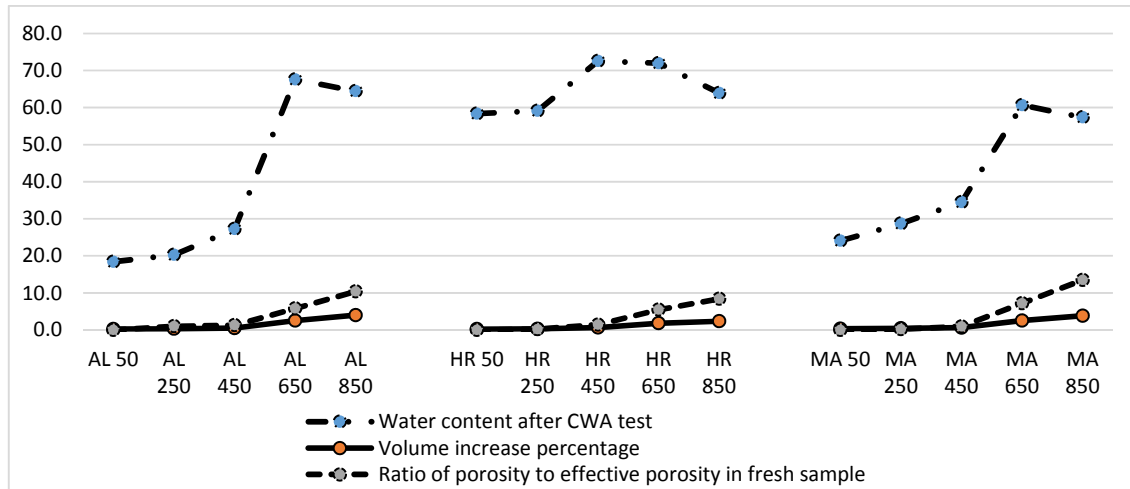
is above 500°C.

Fig. 14 shows the development process of porosity, in other words, the conversion of total porosity to effective porosity. Interesting points are distinguished by examining the total to-effective porosity ratio in the fresh and thermal-shocked samples. The general trend of the diagram shows the increase in effective porosity due to thermal shock in all three samples, although the increasing trend is different in all three samples (Liu et al., 2022).

In the Alvand sample, the total porosity of thermal-shocked samples increases with increasing thermal shock (very similar to the Marivan sample). Finally, at 850°C thermal shock, it becomes almost four times the fresh sample. While in the Hassan Rebat sample with a completely different process, the total porosity of thermal-shocked samples becomes about eight times the total porosity of the fresh sample. It is of note that the total porosity of Hassan Rabat's fresh sample is about one-third of the other two samples. Therefore, this concluded that the increase in the total porosity is independent of the initial total porosity. Other factors, such as mineralogy and texture in granites, can affect the development of total porosity deriving from the thermal induction of micro-cracks that must investigate further. Generally, the effective porosity in the thermal-shocked samples is higher than the fresh ones, but at different thermal shocks, each one shows different behavior from the other. In Alvand granite, the effective porosity is sensitive to thermal shock, and the effective porosity increase from the first stages of thermal shock. In all thermal shocks, the ratio of the effective porosity of thermal-shocked samples to the effective porosity of fresh samples is more than one, i.e., the cracks development and the connection of the micro-crack network starts from the 250°C thermal shock and reaches 15 times the fresh samples with an increasing trend in the 850°C thermal-shock. However, in the samples of Marivan and Hassan Rebat in 250°C thermal shock, the ratio between the thermal-shocked samples' effective porosity to fresh ones is just one, i.e., 250°C thermal shock cannot create a new network of micro-cracks, or cannot create a connected network of total porosity in the rock. Therefore, the effective porosity of thermal-shocked samples is not increased compared to the fresh ones. The ascending trend of the effective porosity starts from 450°C of thermal shock in these two samples and reaches about ten times the fresh samples.

Another significant point is the ratio between total and effective porosity at any thermal-shock. Although the total and effective porosity of both increases due to thermal shock, their increase processes are distinct in various samples. In the Alvand granite sample, the total porosity increases with less acceleration, and the ratio of the total porosity to the effective in 850°C thermal-shocked samples is equal to 1.4, while it is 5 in the fresh sample. Therefore, the development of effective porosity has surpassed, which causes reducing of the ratio of total porosity to effective porosity in the Alvand sample. But, such a trend does not exist in the Hassan Rebat sample. In it, the total and effective porosity develops simultaneously and uniformly and maintains an approximate ratio of 1.2 at all thermal shocks. Marivan sample at 250°C thermal shock maintained the ratio of 3.3. Still, at the higher thermal shock, the development of effective porosity is faster than the total porosity, and the reduction of this ratio begins, which eventually reaches 1.4 at 850°C thermal shock.

Fig.15 shows the volume increase rate and the moisture increase in the samples after the capillary test. But the saturation degree in granites is quite different. The saturation degree obtained after the capillary absorption test is a perfect indicator of the micro-cracks development that absorb and retain water. Micro-cracks less than 0.1  $\mu\text{m}$  in diameter do not absorb water (Tomasic et al., 2011; Winkler, 1997). Micro-cracks with a cross-section of 2 to 6  $\mu\text{m}$  have an adsorption velocity and water absorption capacity up to a height of 10 to 30 m. In this respect, increasing the diameter reduces the absorption capacity, and water absorption accelerates in the horizontal direction twice as fast as in the vertical direction (Tomasic et al., 2011). Considering that the increase in volume indicates an increase in the number and width of micro-cracks, this issue can be attributed to the saturation degree of granite samples.



**Figure 15.** Compare between degree of saturation in samples before & after thermal shock. (Alvand granite AL – Hassan Rebat granite HR – Marivan granite MA)

In all three samples, volume increases as the temperature in a thermal shock increases (Gao et al., 2022; Zhang et al., 2016). The degree of saturation in the Alvand sample shows that in the thermal-shocked sample (850°C), micro-cracks became wider, and the amount of capillary absorption decreased, but the number of micro-cracks was still significantly higher than 450°C thermal shock. The same trend is observed in the Marivan sample. The capillary absorption rate in the Hassan Rebat sample at 250°C thermal shock is very close to the fresh sample, and the development of micro-cracks, or in other words, effective porosity at 450°C and 650°C thermal shock is equal but more than fresh samples. But at 850°C thermal shock, the degree of saturation decreases, and the widening of the cracks and the inability to retain water is a reasons for this (Griffiths et al., 2017; Zhang et al., 2021).

Another point that can interpret from the comparison of diagrams is that since the effective porosity and total porosity in the Hassan Rebat sample developed in the same ratio due to thermal shock, the difference between the saturation degree of the fresh and thermal-shocked samples in this granite is little. But in the other two granite samples, this difference is very significant. Therefore, in different granites, a connected network of microcracks is not necessarily formed due to thermal shock. Individual micro-cracks in the Hassan Rebat sample that did not considerably affect increasing effective porosity and capillary water absorption are examples of this phenomenon.

### Cracks development and speed of sound

As the thermal shock temperature increases, the cracks development increases (Isaka et al., 2018), which is displayed in reducing of  $V_p$  (Liu et al., 2022; Vázquez et al., 2010; Kahraman, S. A. İ. R., 2001; Costa et al., 2021; Gao et al., 2022; Zhang et al., 2016). This method is one of the recommended, very suitable, and non-destructive methods for estimating micro-crack development, whether connected or not (Nicco et al., 2018; Swanson et al., 2020). Fig16, 17, and 18 show this result in all three granite samples.

### Conclusion

P-wave velocity determination and capillary absorption tests performed on thermal-shocked samples showed that the thermal shock, even in one cycle, could significantly affect granites (Liu et al., 2022; Zhao et al., 2020).



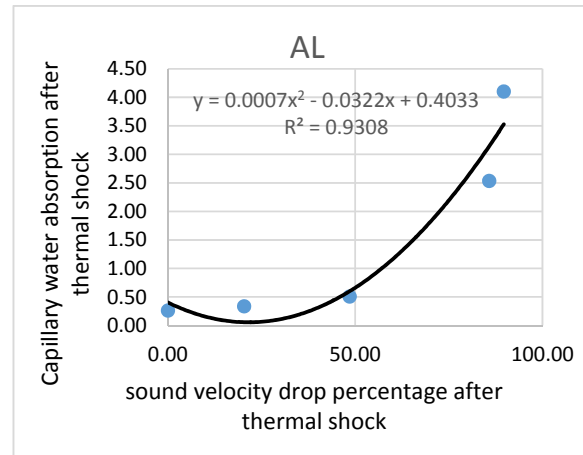


**Figure 16.** Capillary water absorption & sound velocity drop percentage after different thermal shock in Alvand granite

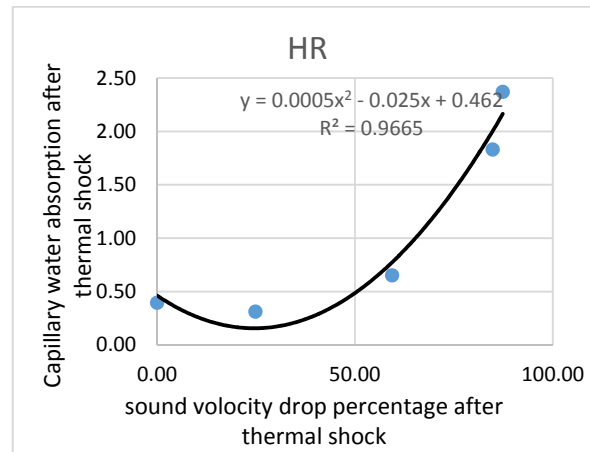


**Figure 17.** Capillary water absorption & sound velocity drop percentage after different thermal shock in Hasan Rebat granite

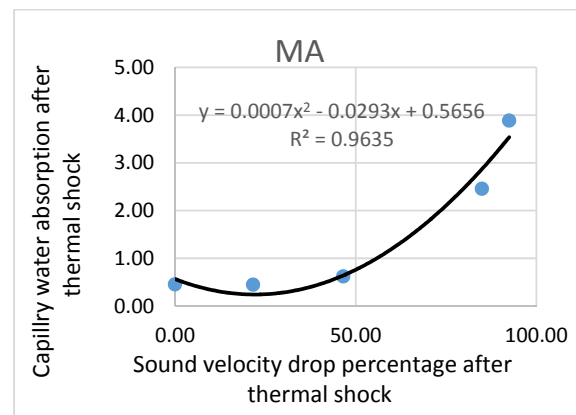


**Figure 18.** Capillary water absorption & sound velocity drop percentage after different thermal shock in Marivan granite

Since thermal shock was performed in only one cycle, it was recognized as a suitable index to evaluate the effect of thermal shock on the physical properties of granite samples. This study showed that increasing the thermal shock up to 500°C has little effect on the physical properties of granite samples, but the thermal shock above 500°C has significant effects on granites (Khan

& Sajid, 2023). An increase in volume was observed in granites as the increase in thermal shock. The P-wave velocity test can well assess the cracks development and micro-cracks due to the thermal shock. An increase in the thermal shock temperature decreases the  $V_p$  in the samples, and the  $V_p$  drop indicates the expansion of micro-cracks. The capillary water absorption test shows how much capillary micro-cracks have formed in the samples, the saturation degree at the end of the capillary test is an indicator of this. The rate of capillary water absorption is also affected by the development of micro-cracks in the horizontal direction. This study showed that the change and increase of porosity are independent of the initial porosity of granites and are affected by other factors that must investigate. In cases where the permeability of granite rocks plays an important role, rising temperature and thermal shock, even in one cycle, can lead to the development of micro-cracks (Liu et al., 2022; Zhao et al., 2020). As the temperature of thermal shock increases, the total and effective porosity increases. However, micro-crack development does not mean they are connected or related to each other, and the total porosity development does not lead to an increase in effective porosity.

## References

- Alm, O., Jaktlund, L.L., Shaoquan, K., 1985. The influence of microcrack density on the elastic and fracture mechanical properties of Stripa granite. *Physics of the Earth and Planetary Interiors*, 40: 161-179.
- Aman, M., Espinoza, D.N., Ilgen, A.G., Major, J.R., Eichhubl, P., Dewers, T.A., 2018. CO<sub>2</sub>-induced chemo-mechanical alteration in reservoir rocks assessed via batch reaction experiments and scratch testing. *Greenhouse Gases: Science and Technology*, 8: 133-149.
- Blake, O.O., Faulkner, D.R., 2016. The effect of fracture density and stress state on the static and dynamic bulk moduli of Westerly granite. *Journal of Geophysical Research: Solid Earth*, 121: 2382-2399.
- Chaki, S., Takarli, M., Agbodjan, W.P., 2008. Influence of thermal damage on physical properties of a granite rock: porosity, permeability and ultrasonic wave evolutions. *Construction and Building Materials*, 22: 1456-1461.
- Chandrasekharam, D., Pabasara Kumari, W.G., Avanthi Isaka, B.L., Gamage, R.P., Rathnaweera, T.D., Anne Perera, M.S., 2018. An influence of thermally-induced micro-cracking under cooling treatments: Mechanical characteristics of Australian granite. *Energies*, 11: 1338.
- Costa, K. O. B., Xavier, G. C., Marvila, M. T., Alexandre, J., Azevedo, A. R. G., Monteiro, S. N., 2021. Influence of high temperatures on physical properties and microstructure of gneiss. *Bulletin of Engineering Geology and the Environment*. 80(9): 7069-7081.
- Darot, M., Gueguen, Y., Baratin, M.L., 1992. Permeability of thermally cracked granite. *Geophysical Research Letters*, 19: 869-872.
- Fahimifar, A., Soroush, H., 2001. Rock mechanic test: theoretical aspects and standards. A Publication of Amirkabir University of Technology, 719 pp. (in Persian)
- Freire-Lista, D.M., Fort, R., Varas-Muriel, M.J., 2016. Thermal stress-induced microcracking in building granite. *Engineering geology*, 206: 83-93.
- Gao, J., Fan, L., Xi, Y., Du, X. 2022. Effects of cooling thermal shock on the P-wave velocity of granite and its microstructure analysis under immersion in water, half immersion in water, and near-water cooling conditions. *Bulletin of Engineering Geology and the Environment*, 81(1): 1-13.
- Ge, S., Shi, B., Zhang, S., Zhai, X., Wu, C., 2022. Thermal damage and mechanical properties of high temperature sandstone with cyclic heating-cooling treatment. *Bulletin of Engineering Geology and the Environment*, 81(7): 1-13.
- Gomah, M. E., Li, G., Bader, S., Elkarmoty, M., Ismael, M. 2021. Damage evolution of granodiorite after heating and cooling treatments. *Minerals*, 11(7): 779.
- Gomah, M. E., Li, G., Sun, C., Jiahui, X., Sen, Y., Jinghua, L., Elkarmoty, M., 2022. Macroscopic and microscopic research on Egyptian granodiorite behavior exposed to the various heating and cooling strategies. *Geomechanics and Geophysics for Geo-Energy and Geo-Resources*, 8(5): 1-22.
- Griffiths, L., Heap, M.J., Baud, P., Schmittbuhl, J., 2017. Quantification of microcrack characteristics

- and implications for stiffness and strength of granite. *International Journal of Rock Mechanics and Mining Sciences*, 100: 138-150.
- Guo, T.Y., Wong, L.N.Y., Wu, Z., 2021. Microcracking behavior transition in thermally treated granite under mode I loading. *Engineering Geology*, 282: 105992.
- Homand-Etienne, F., Houpert, R., 1989. Thermally induced microcracking in granites: characterization and analysis. In *International Journal of Rock Mechanics and Mining Sciences & Geomechanics Abstracts*, 26: 125-134. Pergamon.
- Isaka, B.L.A., Gamage, R.P., Rathnaweera, T.D., Perera, M.S.A., Chandrasekharam, D., Kumari, W.G.P., 2018. An influence of thermally-induced micro-cracking under cooling treatments: mechanical characteristics of Australian granite. *Energies*, 11: 1338.
- Kahraman, S. A. İ. R., 2001. Evaluation of simple methods for assessing the uniaxial compressive strength of rock. *International Journal of Rock Mechanics and Mining Sciences*, 38(7): 981-994.
- Khan, H., Sajid, M., 2023. Investigating the textural and physico-mechanical response of granites to heat treatment. *International Journal of Rock Mechanics and Mining Sciences*, 161: 105281.
- Kumari, W.G.P., Beaumont, D.M., Ranjith, P.G., Perera, M.S.A., Isaka, B.A., Khandelwal, M., 2019. An experimental study on tensile characteristics of granite rocks exposed to different high-temperature treatments. *Geomechanics and Geophysics for Geo-Energy and Geo-Resources*, 5: 47-64.
- Liu, H., Zhang, K., Liu, T., Cao, H., Wang, Y., 2022. Experimental and numerical investigations on tensile mechanical properties and fracture mechanism of granite after cyclic thermal shock. *Geomechanics and Geophysics for Geo-Energy and Geo-Resources*, 8(1): 1-22.
- Meng, Q. B., Qian, W., Liu, J. F., Zhang, M. W., Lu, M. M., Wu, Y., 2020. Analysis of triaxial compression deformation and strength characteristics of limestone after high temperature. *Arabian Journal of Geosciences*, 13(4): 1-14.
- Nara, Y., Morimoto, K., Yoneda, T., Hiroyoshi, N., Kaneko, K., 2011. Effects of humidity and temperature on subcritical crack growth in sandstone. *International Journal of Solids and Structures*, 48: 1130-1140.
- Nasser, M.H.B., Schubnel, A., Young, R.P., 2007. Coupled evolutions of fracture toughness and elastic wave velocities at high crack density in thermally treated Westerly granite. *International Journal of Rock Mechanics and Mining Sciences*, 44: 601-616.
- Nicco, M., Holley, E. A., Hartlieb, P., Kaunda, R., Nelson, P. P., 2018. Methods for characterizing cracks induced in rock. *Rock Mechanics and Rock Engineering*, 51(7): 2075-2093.
- Nicco, M., Holley, E.A., Hartlieb, P., Pfaff, K., 2020. Textural and mineralogical controls on microwave-induced cracking in granites. *Rock Mechanics and Rock Engineering*, 53: 4745-4765.
- Olasolo, P., Juárez, M. C., Morales, M. P., Liarte, I. A. 2016. Enhanced geothermal systems (EGS): A review. *Renewable and Sustainable Energy Reviews*, 56: 133-144.
- Ortega, O., Marrett, R., 2000. Prediction of macrofracture properties using microfracture information, Mesaverde Group sandstones, San Juan basin, New Mexico. *Journal of Structural Geology*, 22: 571-588
- Rossi, E., Kant, M.A., Madonna, C., Saar, M.O., von Rohr, P.R., 2018. The effects of high heating rate and high temperature on the rock strength: feasibility study of a thermally assisted drilling method. *Rock Mechanics and Rock Engineering*, 51: 2957-2964.
- Sano, O., Kudo, Y., 1992. Relation of fracture resistance to fabric for granitic rocks. *Pure and Applied Geophysics*, 138: 657-677.
- Siegesmund, S., Sousa, L. Knell, C., 2018. Thermal expansion of granitoids. *Environmental Earth Science*, 77(2):1-29.
- Sousa, L.M., del Río, L.M.S., Calleja, L., de Argandona, V.G.R., Rey, A.R., 2005. Influence of microfractures and porosity on the physico-mechanical properties and weathering of ornamental granites. *Engineering geology*, 77: 153-168.
- Swanson, E., Wilson, J., Broome, S., Sussman, A., 2020. The Complicated Link Between Material Properties and Microfracture Density for an Underground Explosion in Granite. *Journal of Geophysical Research: Solid Earth*, 125. e2020JB019894.
- Takemura, T., Golshani, A., Oda, M., Suzuki, K., 2003. Preferred orientations of open microcracks in granite and their relation with anisotropic elasticity. *International Journal of Rock Mechanics and Mining Sciences*, 40: 443-454.

- Tomašić, I., Lukić, D., Peček, N., Kršinić, A., 2011. Dynamics of capillary water absorption in natural stone. *Bulletin of Engineering Geology and the Environment*, 70: 673-680.
- Vázquez, P., Alonso, F.J., Esbert, R.M., Ordaz, J., 2010. Ornamental granites: Relationships between p-waves velocity, water capillary absorption and the crack network. *Construction and Building Materials*, 24: 2536-2541.
- Wang, P., Xu, J., Liu, S., Wang, H., Liu, S., 2016. Static and dynamic mechanical properties of sedimentary rock after freeze-thaw or thermal shock weathering. *Engineering Geology*, 210: 148-157.
- Winkler, E.M., 1997. Physical Properties of Stone. In *Stone in Architecture*. pp. 32-62. Springer, Berlin, Heidelberg.
- Wong, L. N. Y., Zhang, Y., & Wu, Z., 2020. Rock strengthening or weakening upon heating in the mild temperature range? *Engineering Geology*, 272: 105619.
- Xu, C., Sun, Q., Pan, X., Zhang, W., Wang, Y., 2019. Variation on thermal damage rate of granite specimen with thermal cycle treatment. *High Temperature Materials and Processes*, 38(2019): 849-855.
- Yin, T., Li, Q., Li, X., 2019. Experimental investigation on mode I fracture characteristics of granite after cyclic heating and cooling treatments. *Engineering Fracture Mechanics*, 222: 106740.
- Yu, L., Peng, H. W., Zhang, Y., Li, G. W., 2021. Mechanical test of granite with multiple water-thermal cycles. *Geothermal Energy*, 9(1): 1-20.
- Zhang, F., Zhang, Y., Yu, Y., Hu, D., Shao, J., 2020. Influence of cooling rate on thermal degradation of physical and mechanical properties of granite. *International Journal of Rock Mechanics and Mining Sciences*, 129: 104285.
- Zhang, W., Shi, Z., Wang, Z., Zhang, S. 2021. Identifying critical failure information of thermal damaged sandstone through acoustic emission signal. *Journal of Geophysics and Engineering*, 18(4): 558-566.
- Zhang, W., Sun, Q., Hao, S., Geng, J., Lv, C., 2016. Experimental study on the variation of physical and mechanical properties of rock after high temperature treatment. *Applied Thermal Engineering*, 98: 1297-1304.
- Zhao, G., Hu, Y., Jin, P., 2020. Exploratory Experimental Study on the Mechanical Properties of Granite Subjected to Cyclic Temperature and Uniaxial Stress. *Energies*, 13(8): 2061.
- Zhu, S., Zhang, W., Sun, Q., Deng, S., Geng, J., Li, C., 2017. Thermally induced variation of primary wave velocity in granite from Yantai: experimental and modeling results. *International Journal of Thermal Sciences*, 114: 320-326.

